

Enhanced thermal properties of phthalonitrile networks by cooperating phenyl-s-triazine moieties in backbones



Lishuai Zong, Cheng Liu, Shouhai Zhang, Jinyan Wang^{*}, Xigao Jian

State Key Laboratory of Fine Chemicals, Department of Polymer Science and Materials, School of Chemical Engineering, Dalian University of Technology, Dalian 116024, China

ARTICLE INFO

Article history:

Received 23 April 2015
Received in revised form
7 September 2015
Accepted 15 September 2015
Available online 16 September 2015

Keywords:

Phenyl-s-triazine
Phthalonitrile resins
Composite laminates

ABSTRACT

The development of phthalonitrile resins is of particular interest for aerospace applications because of their excellent heat resistance. Here, heteroaromatic phenyl-s-triazine moieties have been introduced into the architecture of the phthalonitrile resin as thermally stable segments via a two-step, one-pot reaction. Bis(4-[4-aminophenoxy]phenyl)sulfone was selected to promote the curing reaction, and the gelation time could be readily controlled by the diamine concentration and the curing temperature as evidenced by rheometric measurements. The curing procedure was optimized to give high cross-linking density networks. The resulting networks exhibit high glass transition temperatures at around 400 °C, outstanding thermo-oxidative stability with weight retention of 95% ranging from 539 °C to 552 °C, suggesting an improvement of the thermal properties imposed by phenyl-s-triazine units. Additionally, the CF laminate of the resin possesses high flexural strength of 1722 MPa and interlaminar shear strength of 71 MPa at ambient temperature, and these values retain 255 MPa and 36 MPa at 450 °C, respectively.

© 2015 Elsevier Ltd. All rights reserved.

1. Introduction

Great efforts have recently been devoted to high-performance materials facing aerospace industry mainly due to their high modulus and strength to weight ratios [1]. One of the increasingly demanding requirements for these materials is used in heat-resistance components of aerospace vehicles such as the space shuttle and reentry module. Phthalonitrile resins, as an emerging high-performance material [2], have opened up a new possibility to meet this requirement because of possessing a combination of promising properties including excellent thermal properties, superior flame and chemical resistance, less flaming smog, and facile preparation [3].

Pioneering study on phthalonitriles for high-temperature materials was disclosed by Marvel and coworkers [4]. Unfortunately, few attempts were performed on phthalonitrile resins until 1970s [5]. Keller and coworkers have prepared a number of phthalonitrile monomers and polymers, featuring random lengths of oligomeric aromatic ether spacer units between curable terminal groups [6]. The networks were obtained by thermally induced curing under

moderately elevated conditions. They are all associated with high 5% mass loss temperature and char yield at 1000 °C [7], and could be used as the competitive high-performance materials for marine and aerospace applications [8]. Since the condition of curing neat phthalonitriles was extremely sluggish [9], curing additives were utilized to accelerate the cross-linking reaction. Among kinds of curing additives, e.g., metals [10], metallic salts [11], organic acids [3c], phenols [12], amines [13], and bispropargyl ether [14], diamines are more extensively used [6a,15]. Two factors have been taken into account. First, amine-cured polymers are considered more thermally stable than other cured counterparts. This can be ascribed to the robust interaction between amines and phthalonitriles, which favorably leads to higher degree of polymerization. Second, amines could also moderately react with phthalonitriles. Thus, tailoring the type of diamines as well as their concentration and the curing temperature could readily control the melt viscosity of the curing system. This undoubtedly facilitates the processing of the resins.

On the other hand, a tremendous amount of efforts has been currently focused on a rational design of the structure of phthalonitrile polymers. For instance, sterically rotatable *meta*, *ortho*-position bisphenoxy moieties [16] along with flexible alkyl-center-trisphenoxy [13b] and silane [17] structures were separately introduced to bind with phthalonitrile groups to generate

^{*} Corresponding author. Tel.: +86 41184986109.
E-mail address: wangjinyan@dlut.edu.cn (J. Wang).

monomers with low-melting point, wide processing window and excellent thermal properties. These monomers were competent to face more cost-effective processing methods such as resin transfer molding (RTM), resin infusion molding (RIM), and vacuum-assisted resin transfer molding (VARTM). Combined all the merits displayed by phthalonitriles, incorporating curable phthalonitrile units is widely deemed as a possible approach for tailoring the comprehensive properties of the known commercial resins (e.g. Epoxy [18], Benzoxazine [19], Novolac [20], Poly(aryl ether)s [20d,21], Polyamide [22], and Polyimide [23]) by many researchers. This strategy has been already accomplished through either chemical modification or physical blending method, and the resulting thermosetting polymers are proved attractive for advanced technological applications including composites, adhesives, electronic conductors, magnetic and microwave absorption materials [24]. However, these works neglect to incorporate thermally stable and high-stiff groups into phthalonitrile-based polymer backbones. Such groups may enhance the stability and stiffness of the polymer main chain, in turn to bring about the increase for the heat resistance of the cross-linked product.

Inspired by this concept, our previous work demonstrated the preparation of the phthalazinone-bearing monomers [25], poly(arylene ether amide)s [26], poly(arylene ether imide)s [27] as well as poly(arylene ether nitrile)s [28] terminated with cyano groups, subsequently reporting their trimerization to high-performance s-triazine resins. The twisted, non-coplanar phthalazinone structures in the polymer's main chain endow the polymers high thermal stability and good solubility.

In this paper, we furthered this concept for pursuing ultrahigh performance phthalonitrile polymers with the aid of phenyl-s-triazine units. s-Triazine units, one of the most thermally stable heteroatomic ring reported, were manifested having strong charge transfer interaction between s-triazine ring and aromatic ring inside [29]. This would undoubtedly enhance the rigidity of the polymer backbone. According to previous reports, the synthesis of the monomers containing phenyl-s-triazine segment suffer from toxic and irritant smelling SO_3 or NH_3 and low yield [30]. Alternatively, we presented herein a facile one-step synthetic strategy to generate phenyl-s-triazine-containing monomer, namely 2-phenyl-4,6-bis(4-fluorophenyl)-1,3,5-triazine (**1**). A phenyl-s-triazine-containing phthalonitrile oligomer was subsequently designed and prepared (named as **5**). The kinetics of curing reaction, melting behaviors and curing procedure of **5** cured with bis[4-(4-aminophenoxy)phenyl]sulfone (named as **6**) were investigated in details. The thermal stabilities of the resultant resins (named as **7**) are significantly modified by the introduction of phenyl-s-triazine moieties and increase on the addition of **6** for 2–10 wt % loading. Simultaneously, the resins exhibit limited water absorption capability, which is also closely related to the % **6** inclusion. The carbon fiber (CF) reinforced composite of the 5 wt % hybrid was fabricated. The result of the mechanical tests indicated that this type of phthalonitrile resin might be potentially used as structural matrix resin for high-performance applications.

2. Experimental

2.1. Materials

4,4'-Biphenol (BP, 99%, **2**), bis(4-chlorophenyl)sulphone (BCS, 99%) and 4-aminophenol (APO, 99%) were purchased from Haiqu chemical Co., Shanghai, China. 4-Fluoro-benzonitrile (FBN, 99%) and 4-nitro-phthalonitrile (NPH, 99%, **4**) were purchased from Jiakailong chemical Co., Wuhan, China. Benzaldehyde (BA, A.R.), chlorobenzene (CB, A.R.), toluene (A.R.) and other solvents were purchased from Kermel Chemical Reagent Co., Ltd., Tianjin, China.

Aluminum(III) chloride (AlCl_3 , A.R.) and Ammonium chloride (NH_4Cl , A.R.) were purchased from Bodi Chemical Reagent Co., Ltd., Tianjin, China. All chemicals and solvents above were used without further purification. Anhydrous potassium carbonate (K_2CO_3 , 99%, Beijing Chemical Co., China.) was ground and dried in vacuum at 100 °C for 24 h before used. N-methyl pyrrolidone (NMP, A.R., Kermel Chemical Reagent Co., Ltd., Tianjin, China.) was refluxed with CaH_2 for 2 h, and then vacuum distilled. The 125–127 °C boiling range fraction was collected and stored over molecular sieves (type 4 Å). T300 CF fabric was provided by Aviation Industry Corporation of China (AVIC). T700 continuous CF was purchased from TORAY and disposed at 350 °C for 5–10 min before used.

Bis[4-(4-aminophenoxy)phenyl]sulfone (BAPS, **6**) was prepared according to described work by Barikani [31]. The product was recrystallized from toluene, and brown flaky crystal was obtained. Purity: 99 wt %. APCI/MS ($\text{M} + \text{Calcd. as } \text{C}_{21}\text{H}_{13}\text{N}_2\text{F}_2$: $m/z = 432.11$): $m/z = 432.00$ (M^+).

2.2. Methods and equipment

High performance liquid chromatography (HPLC) was performed on a Hewlett–Packard (HP) 1100 liquid chromatograph using a mixture of acetic acid (0.1 wt%) and methanol (v/v ¼ 90:10) as eluting solvent and a 2.0×150 mm Microbore column (Waters Spherisorb® S5 ODS2) as column. Inherent viscosities (η_{inh}) of the polymers were measured using an Ubbelohde capillary viscometer at a concentration of 0.5 g dL^{-1} in NMP at 25 °C. Fourier transform infrared (FT-IR) measurements were performed with a Thermo Nicolet Nexus 470 FT-IR spectrometer. ^1H NMR (400 MHz), ^1H – ^1H gCOSY NMR (400 MHz) and ^{13}C NMR (100 MHz) spectra were recorded with a Varian Unity Inova 400 spectrometer using CDCl_3 or CDCl_3 and CF_3COOD mixed solvents and listed in parts per million downfield from tetramethylsilane (TMS). Matrix-assisted laser desorption ionization time-of-flight mass spectroscopy (MALDI-TOF-MS) analyses were performed on a Micromass GC-TOF CA 156 MALDI-TOF/MS. Elemental analyses were conducted on a Vario ELIII CHNOS Elementaranalysator from Elementar-analysesysteme GmbH for C, H, N, and S determinations. Gel permeation chromatography (GPC) analysis was carried out on an Agilent PL-GPC 50 Intergrated GPC system equipped with two PLgel 5 μm MIXED-C columns (300×7.5 mm) arranged in series with NMP as solvent calibrated with polystyrene standards. The solubility test was performed by dissolving 0.04 g oligomer in 1 mL solvent (4%, w/v) at different temperatures. The thermal properties of the obtained materials were determined using a modulated TA Q20 instrument at a heating rate of 10 °C/min under a nitrogen flow of 50 mL/min. The kinetics study of the reaction between **5** and **6** (5 wt %) was conducted by the non-isothermal DSC method at the heating rate of 5, 10, 15, and 20 °C/min. The samples were prepared by thoroughly grounding for three times to ensure homogeneity. The DSC tests of the cured **7s** was evaluated at the heating rate of 20 °C/min. Rheological behavior was investigated using a TA AR2000 instrument under a frequency of 1 Hz and a strain of 0.02 N. The sample was compacted into a flaky cylinder with the dimension of $\Phi 25 \times 1 \text{ mm}^3$ in advance. Dynamic mechanical analysis (DMA) measurements were carried out with a TA Q800 instrument at 1 Hz and a heating rate of 3 °C/min from 25 °C to 400 °C under air atmosphere using a $30 \times 10 \times 2 \text{ mm}^3$ T300 composite sample, in order to characterize the dynamic mechanical spectra including mechanical damping $\tan \delta$, storage modulus E' and loss modulus E'' . Thermal Gravimetric Analysis (TGA) was obtained from a TA Q500 instrument at a heating rate of 20 °C/min $^{-1}$ in N_2 or air. The gel contents of the cured samples were studied according to ASTM D2765-11 standard. NMP was selected as the extracting solvent. The oxidative stability was performed via

handling a 0.5 g sample in a muffle furnace at various temperatures (250–450 °C) each for 8-h intervals under static air atmosphere. The retention weights for every temperature step were recorded. The long-term water absorptions were studied based on ASTM D570-98 standard. The flexural strength and interlaminar shear strength were determined using an Instron-5869 machine with a capacity of 500 N on T700 composite samples according to ASTM D790-10 and ISO 14130 standards, respectively. The high-temperature (450 °C) mechanical properties were achieved on-line via a peripheral heating oven. The resin content of the composite (T700) was measured according to ASTM D3171-15 standard. Annex A7 procedure was used to digest the matrices at 600 °C, and a paralleled sample of carbon fiber was heated simultaneously for calculating the original mass of the carbon fiber in the composite. SEM studies were performed on the cracked section of the composite with a FEI QUANTA 450 instrument at 15 kV.

2.3. Synthesis of 2-phenyl-4,6-bis(4-fluorophenyl)-1,3,5-triazine (BFPT, **1**)

A facile one-step procedure is shown as follows (Scheme 1): To a stirred solution of FBN (0.10 mol, 12.111 g), BA (0.05 mol, 5.1 mL) and NH₄Cl (0.05 mol, 2.675 g) in CB (100 mL) was added AlCl₃ (0.05 mol, 6.667 g) progressively at an ice-bath temperature (−5 to 0 °C). Then the ice bath was removed. The yellow solution was gradually heated to 130 °C and maintained at this temperature for 8–12 h. The product was precipitated by slowly pouring the mixture into an ice-containing 5% aqueous HCl solution. CB was removed via steam distillation. The material was collected using Büchner funnel and rinsed with distilled water until neutral. Then, the obtained white solid was added into a 250 mL of three-necked flask, and stirred with 200 mL methanol. The suspension was filtered, and the crude product was dried at 100 °C under vacuum for 24 h. Finally, the product was recrystallized from toluene, white long thin needle crystal was obtained, which should be ground before used. Yield: 82%, m.p.: 260.2–260.8 °C; purity: 99 wt %. MALDI-TOF/MS (M + Calcd. as C₂₁H₁₃N₂F₂ 345.1078): m/z = 345.1067(M+). ¹H NMR (400M, CDCl₃): δ 8.91–8.61 (m, 6H), 7.74–7.50 (m, 3H), 7.39–7.12 (m, 4H).

2.4. Synthesis of oligomer **5**

As Scheme 2 shows, to a 250 mL three-necked flask equipped with a Dean-Stark trap with a nitrogen inlet was added **2** (0.06 mol, 11.189 g), K₂CO₃ (0.08 mol, 11.057 g), 30 mL NMP and 30 mL toluene. The mixture was stirred at room temperature for 5 min, and then the temperature was raised gradually to 140 °C under a nitrogen atmosphere. After the generated water was completely azeotroped off with toluene, the reaction was allowed to cool to room temperature. **1** (0.03 mol, 10.369 g) along with 20 mL NMP was charged into the flask. The system was heated stepwise to 190 °C, and held for 3 h. The obtained solution was then cooled to 50 °C. NPH (0.07 mol, 12.119 g) and 30 mL NMP were added into the flask. The reaction system was heated to 80 °C for 8–10 h. After cooling to room temperature, the resultant brown mixture was poured to a 5% aqueous

NaOH solution. The filtered solid was rinsed continuously with the 5% aqueous NaOH solution until the filtrate turned to colorless. Then the solid was washed with distilled water until neutral. The yield of dried crude product was 92%. Subsequently, the crude product was purified by reprecipitation from NMP into ethanol, and then dried at 120 °C in a vacuum oven for 20 h. The constitutional repeating unit of the target product (**n**) was theoretically designed to be 1 by controlling the feed ratio. The value for **n** of the obtained product was calculated via the terminal group analysis method based on the ¹H NMR spectrum (Fig. S6) [32]. It is approximately 1.8. Total yield: 78%. ¹H NMR (400M, CDCl₃ and CF₃COOD): δ 8.64 (d, J = 13.7 Hz, 2H), 8.54 (d, J = 13.4 Hz, 1H), 7.93–7.79 (m, 1.1H), 7.72 (dd, J = 16.4, 8.1 Hz, 4H), 7.44–7.34 (ss, 1.14H), 7.27 (t, J = 8.8 Hz, 4H), 7.21 (d, J = 8.5 Hz, 1.04H). ¹³C NMR (101 MHz, CDCl₃ + CF₃COOD): δ 167.59 (s), 167.20 (s), 166.03 (d, J = 7.7 Hz), 162.53 (d, J = 6.8 Hz), 160.79 (s), 160.37 (s), 159.96 (s), 159.54 (s), 153.95 (d, J = 17.2 Hz), 153.02 (d, J = 16.4 Hz), 137.76 (s), 137.44 (s), 136.79 (s), 175.83–103.05 (m), 136.00 (s), 133.44 (s), 130.12 (s), 129.76 (s), 129.59–128.61 (m), 123.35 (s), 121.97 (d, J = 12.1 Hz), 121.13 (d, J = 11.8 Hz), 118.84 (s), 118.05 (s), 116.89 (s), 116.01 (s), 114.83 (s), 114.36 (s), 113.17 (s), 110.33 (s), 107.54 (d, J = 4.7 Hz).

2.5. Curing procedure for the formation of the networks (**7**)

The formation of the networks (**7**) was typically achieved by a thermally induced procedure as follows (Scheme 2). To 1.0 g oligomer **5** was added 0.02–0.1 g **6** (2–10 wt %). The mixture was thoroughly grounded, and then the well-mixed sample was compressed to a void-free flaky cylinder (Φ 25 × 2 mm³) under elevated pressure. The sample was thermally cured by heating in an oven at 250 °C/3 h + 285 °C/1 h + 325 °C/3 h + 350 °C/2 h + 375 °C/8 h to afford the cross-linked polymer. Then, a portion of **7** was pulverized and used for DSC and TGA analysis. The residual bulky sample was used for long-term oxidative stability and water-uptake studies.

2.6. Fabricating process of the 7/T700 composite

The network **7** containing 5 wt % **6** was selected to fabricate the composite (T700). To a three-necked flask was charged 50 g **5**, and then the flask was heated to 250 °C. 2.5 g **6** was added to the melted **5** with vigorous stirring. The mixture was maintained at 250 °C for 7 min, then cooled down. The obtained pre-polymer (B-stage resin) was dissolved in 100 mL NMP. The T700 carbon filament was dipped into the solution, and wound continuously to an iron frame of 300 × 210 mm² (Fig. 1) to afford the unidirectional prepreg. After dried under the infrared lamp, the prepreg was transferred to a vacuum oven, dried at 180 °C for 36 h, 200 °C for 1 h. The solvents have been thoroughly removed as evidenced by TGA (Fig. S3). Then, the prepreg was tailored into 100 × 60 mm² dimension. Twelve tailored prepregs were compacted into a tight steel mold with a pressure of 2.5 MPa at 250 °C for 2 h. Then the steel mold was removed, and the obtained laminate was cured at 250 °C for 1 h, 285 °C for 1 h, 325 °C for 3 h, 350 °C for 2 h, and 375 °C for 8 h in a muffle furnace. The thickness of the finished laminate was approximately 2 mm. It should be sawed and sanded into 80 × 10 × 2 mm³ size and 20 × 10 × 2 mm³ size for flexural strength and interlaminar shear strength tests, respectively. The weight percentage of the fiber of the laminate was 62.7% based on the ASTM D3171-15 standard.

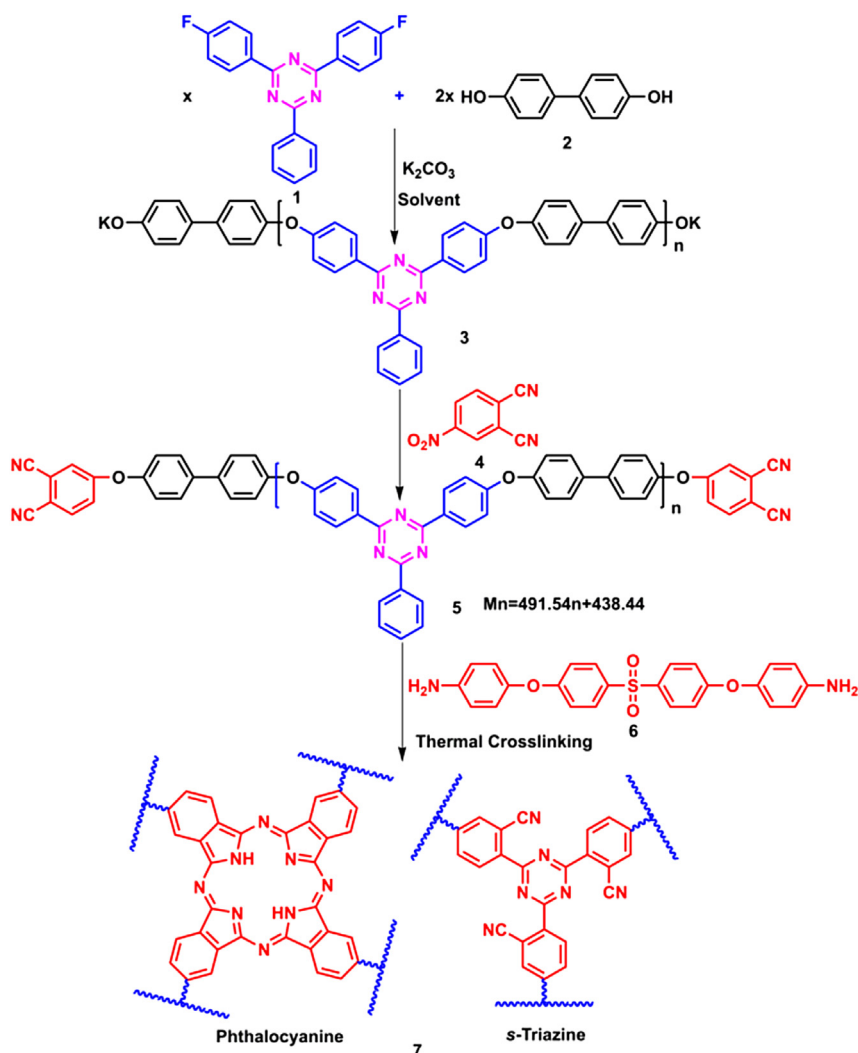
3. Results and discussion

3.1. Synthesis of oligomer **5**

A phthalonitrile-terminated oligomeric poly(aryl ether) (**5**) was



Scheme 1. Synthetic route to **1**.



Scheme 2. Synthetic route of oligomer **5** and subsequent network **7** formation.

successfully prepared by a two-step, one-pot reaction, as [Scheme 2](#) shows. The first reaction step is a typical nucleophilic substitution reaction. An *s*-triazine-activated dihalo compound **1** first reacted with biphenol **2** through a Meisenheimer complex at 190 °C. NMP/toluene solvent system was favorably chosen, because NMP would provide sufficient solubility for the product to ensure the reaction proceeded steadily towards the target product. Toluene would help to azeotrope off the by-product water. Then the toluene was

removed from the system before polymerization. This is contrary to the reported procedure [[7b](#)] and attributed to the limited solubility of intermediate **3** imposed by the steric planarity and the electron affinity of the phenyl-*s*-triazine groups. The presence of toluene may induce **3** precipitated from the reaction solution. Consequently, the resulting product exhibits a broader polydispersity index ([Fig. S3](#)). In the second step, the reaction underwent a milder nitro-substituted reaction at 80 °C for 12 h. An excess amount (5%) of **4** was used to convert the phenolates into the cross-linkable phthalonitrile moieties completely. The relatively synthetic details are summarized in [Table 1](#). As expected, solubility study reveals that **5** is readily soluble in NMP, and also in some less efficient solvents such as tetrachlorethane and hot pyridine ([Table S1](#)). The rational solubility may be resulted from the strongly polar phthalonitrile terminals. These units would be easily polarized by the solvent molecule, and in turn to solubilize the oligomer efficiently. This would substantially make the oligomer **5** competent for composite applications through solution impregnating technology.

3.2. Characterization of oligomer **5**

The MOLDI-TOF/MS spectrum ([Fig. S4b](#)) has provided primary evidence to certify the structure of the resultant **5**, due to the

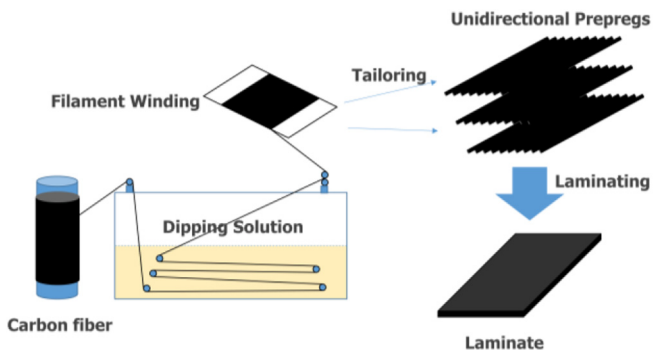


Fig. 1. The schematic diagram for the fabrication of the 7/T700 composite.

Table 1
Synthetic data of Oligomer 5.

Sample	Solvent	Charge ratio (2:1:4)	Temperature (°C)	Time (h)	M_n^a	M_n^b	M_n^c	PD ^c	Yield(%)	η_{inh}^d (gdL ⁻¹)	Color
5	NMP	2:1:2.1	190	3	930	1316	1011	3.69	92	0.013	Gray

^a Designed molar mass controlled by the charge ratio of **2** versus **1**.

^b Number-average molar mass of **5** calculated by the integration area of characteristic peaks through ¹H NMR spectrum in CDCl₃ and CF₃COOD.

^c Number-average molar mass and polydispersity of **5** measured by GPC in NMP.

^d Inherent viscosity of **5** determined at a concentration of 0.5 g/dL in NMP at 25 °C.

correlation between the detected molar mass and the designed values. No trace of hydroxy-terminated oligomer peaks indicates sufficient displacement of the nitro groups by the ether linkages. Detailed analyses of the chemical structure of oligomeric **5** were further performed using instrumental techniques including FT-IR, NMR and ¹H–¹H gCOSY. The FT-IR spectra of oligomer **3** and **5** (Fig. S5) demonstrate the characteristic bands of *s*-triazine group at 1488 cm⁻¹ and 1363 cm⁻¹. The cyano group is located by the stretching band at 2230 cm⁻¹ in the spectrum of oligomer **5**. Compared to the spectrum of **3**, the appearance of the cyano group indicates successful introduction of this cross-linkable moiety into the molecular structure. The exact structure of oligomer **5** was certified by the NMR spectra (Fig. S6–S8). Each discernible shifting peak was accurately assigned with the assistance offered by the ¹H–¹H gCOSY spectrum of oligomeric **5** (Fig. S7). The set of peaks shifting downfield at 8.49–8.72 ppm are attributed to the protons (H5, 6), which are adjacent to *s*-triazine groups (Fig. S6bc). Note that the H5 and H6 shift at different fields with the integral intensity ratio of 2:1 in mixed solvents of CDCl₃ and CF₃COOD (Fig. S6c). These signals can be used as the referenced signals to position the protons (H1–4, 7, 8). The rest protons resonating at 8.32–8.40 ppm are associated with H9, 10 of phthalonitrile moiety. The disappearance of active halogen (O–H) signal (5.23–5.27 ppm, Fig. S6a) confirms the complete transformation of the hydroxyl groups to ether-linked phthalonitrile moieties. Since all the area peaks can be well ascertained, the value of *n*, which represents the number of polymer repeating units, could be calculated via terminal analysis method [32]. The M_n of oligomer **5** was subsequently calculated as 1316 g/mol. The value, higher than the designed molecular mass (930 g/mol), might be caused by the loss of low molar product during the purification procedure, and is in agreement with previous reports [33]. Thus, the characterization study certifies that the proposed phthalonitrile oligomer was successfully synthesized.

3.3. Thermal cure behaviors

The thermal property of the neat oligomer **5** was investigated by DSC up to 400 °C (Fig. 2). In the first heating curve, a slight glass transition appeared at 97 °C, implying a rather low molecular weight (the reported T_g of polymer PAEP is 241 °C) [30a]. Then an endothermic peak was recorded at 211 °C. Such a wide peak is associated with the broad molecular weight distribution (PD = 3.69). When the sample was quenched and reheated immediately, the oligomer showed an increased T_g of 137 °C, accompanied by vanishing of the melting peak. It suggests that **5** experienced a somewhat self-promoting reaction under elevated temperature, which agrees with Keller's analysis [34].

For promoting the curing rate, a small amount (5 wt %) of typically used diamine **6** was combined with **5** during the thermally induced curing process. The non-isothermal DSC tests of **5/6** mixture (Fig. 3) were carried out, followed by elucidating the kinetics of the curing reaction. A significant exothermic peak appears in each DSC trace with the peak temperature of 242, 254, 264, 269 °C for the heating rate of 5, 10, 15, 20 °C/min, respectively.

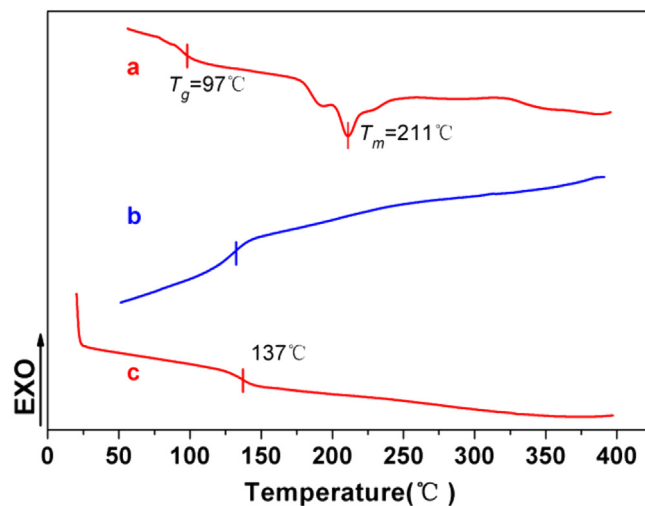


Fig. 2. DSC curves of oligomer **5** under N₂ atmosphere: (a) First run at the heating rate of 10 °C/min; (b) Cooling curve at the cooling rate of 10 °C/min; (c) Second run at the heating rate of 10 °C/min.

Kissinger method [35] was employed to calculate the cure kinetics parameters of the reaction between **5** and **6** (See the analysis details in Supplementary data) [36]. The results are listed in Table S2. The activation energy of the reaction between **5** and **6** (107.7 kJ/mol) is significantly higher than the self-promoted phthalonitrile resins disclosed by Zhou [16a] as well as the well-known Epoxy [37], bismaleimide (BMI) [38], and benzoxazine (BA) resins [1e], implying more energy is entailed to overwhelm the extremely high

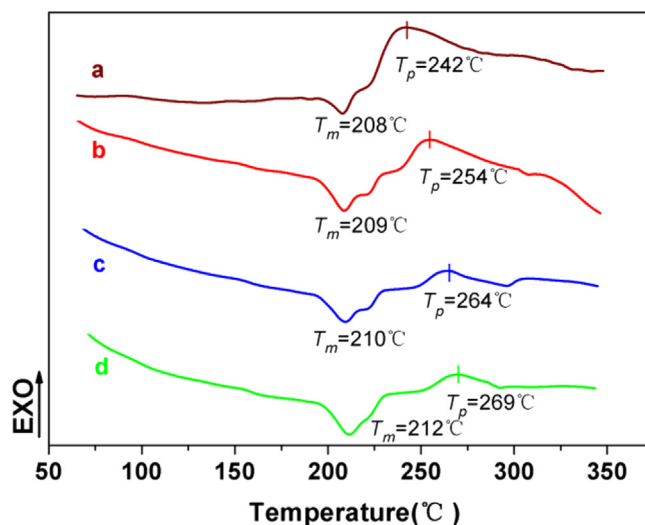


Fig. 3. DSC curves of oligomer **5** with 5 wt % **6** in N₂ atmosphere: (a, b, c, d) first run with the heating rate of 5, 10, 15, 20 °C/min, respectively.

Table 2
Three cure schedules upon **5** with 5 wt % **6** under environmental atmosphere.

Index	Specific procedure
a	250 °C/3h + 285 °C/1h + 325 °C/8h
b	250 °C/3h + 285 °C/1h + 325 °C/3h + 350 °C/8h
c	250 °C/3h + 285 °C/1h + 325 °C/3h + 350 °C/2h + 375 °C/8h

potential barrier, which intuitively behaves as requiring much higher temperature. Additionally, the high frequency factor (A , 2.0×10^{10}) along with the untidy reaction order (n , less than 1) demonstrates a complex curing reaction.

In this context, for pursuing highly cross-linked thermoset resins, three curing schedules were empirically designed to polymerize the oligomer **5** with 5 wt % **6** loading (Table 2). The reaction is initiated by the nucleophilic attack of the amine group to the carbon atom of the nitrile group to generate an iminoisoindolenine-containing compound. Then it reacts with another phthalonitrile group to give chain extension. And after curing at even high temperature, isoindoline, triazine, dehydrophthalocyanine, and phthalocyanine was produced [6a,12a,13a] (Scheme S1). As we know, the well-cured polymers are always associated with attractive properties including high glass transition temperature, excellent thermal stability, and commendable mechanical property. Thus, three set of tests (*i.e.*, DSC, TGA, and flexural strength measurement) for the cured **7** or its CF-reinforced composite were carried out to give the most desirable curing cycle. DSC study (Fig. 4) obviously reveals that the products cured under a and b schedule soften at 179 °C and 212 °C, respectively, due to their low degree of polymerization. Notably, no distinct transition was detected in c-schedule curve, indicating 375 °C curing step is beneficial to the polymerization of phthalonitrile-terminated resin/diamine system, which is consistent with previous research [3a]. Likewise, TGA and DTG tests (Fig. 5) afford similar conclusion. Both the initial decomposition temperatures and the residue mass of thermosetting resin **7**s significantly increase when the curing cycle was used from a to c. DTG data disclose that the temperatures of thermo-gravimetric rate of all the networks peak at 540 °C and 590 °C. The 540 °C peak decreases gradually and eventually disappears, while the 590 °C peak behaves conversely as the final curing temperature was elevated. However, the slight residue of 540 °C peak in c-schedule trace has not escaped our observation, which strongly suggests that an elevated temperature such as 425 °C for curing is necessary. Thus, by post heated at 425 °C for 8 h under static air atmosphere, the network shows 5% mass loss

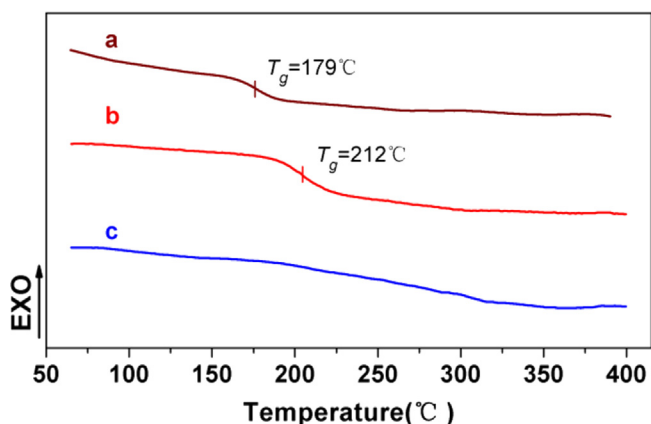


Fig. 4. DSC curves of networks (**7**) separately cured under a, b, c schedule with 5 wt % **6** with the heating rate of 5 °C/min.

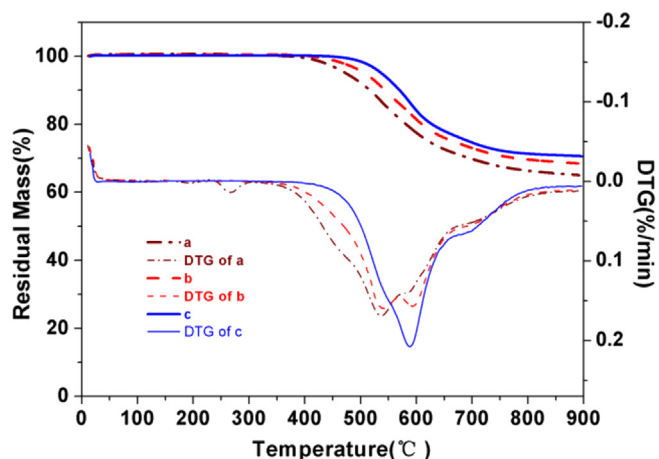


Fig. 5. TGA and DTG curves of networks (**7**) separately cured under a, b, c schedule with 5 wt % **6** with the heating rate of 20 °C/min detected in N_2 .

temperature rising from 537 °C to 565 °C, along with the char yield at 900 °C increasing for 2.5% and the disappearance of the 540 °C peak in DTG curve (Fig. S10). Unfortunately, the high-temperature (425 °C) curing schedule caused a non-negligible mass loss for 6.3%, suggesting that this cross-linking procedure should be cautiously utilized. The flexural strength test of the continuous CF-reinforced laminates of **7** (Fig. 6) also provided effective evidence for choosing the optimal curing cycle. The c-schedule-cured laminate exhibits the highest flexural strength of 1722 MPa as compared to other laminates. As a result, c schedule was convinced as the most suitable procedure for curing the phenyl-*s*-triazine-containing phthalonitrile oligomer/diamine system.

The structure of cured **7** were characterized by FT-IR (Fig. S11), the peak intensity of the nitrile group weakened, and the absorption at 1502, 1360, and 1004 cm^{-1} appeared, both of which indicate the curing of phthalonitrile groups and the formation of phthalocyanine and *s*-triazine structures.

3.4. Meltability and processability

The rheological behavior of the resins is a key factor in determining their processabilities. Therefore, the variation of the

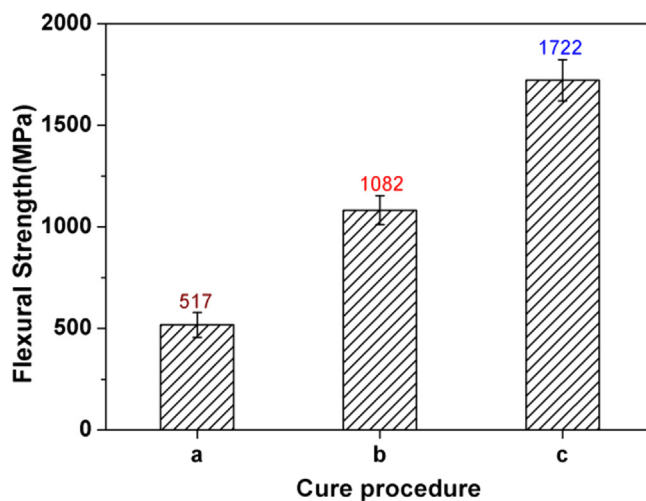


Fig. 6. Flexural strength of the continuous CF-reinforced laminates of **7** separately cured by a, b, c procedures with 5 wt % **6** under air atmosphere according to ASTM D790-10 Standard.

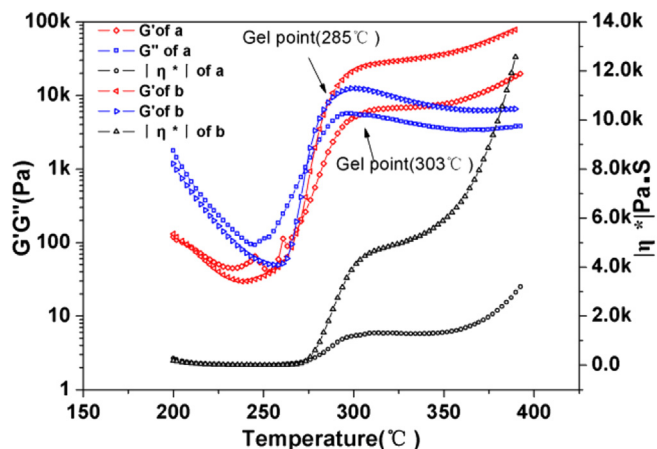


Fig. 7. Storage Modulus (G'), Loss Modulus (G'') and Complex viscosity (η^*) of oligomer **5** as a function of temperature at a heating rate of $3\text{ }^\circ\text{C}/\text{min}$ with 2 wt % (a) and 5 wt % (b) **6**.

complex viscosity of oligomer **5** as a function of temperature was measured from $175\text{ }^\circ\text{C}$ to $400\text{ }^\circ\text{C}$, and the storage modulus and loss modulus were simultaneously recorded. The results (Fig. S12) indicate that the complex viscosity of neat **5** decreased rapidly after melting at about $215\text{ }^\circ\text{C}$, and then reached a minimum for $4.2\text{ Pa}\cdot\text{s}$ at $283\text{ }^\circ\text{C}$. The gelation, which is determined from the crossover point of the storage modulus (G') and the loss modulus (G''), occurred at $303\text{ }^\circ\text{C}$. After this, both of G' and G'' leveled off, indicating that the self-curing reaction proceeded sluggishly. However, the curing process would be promoted in the presence of the additive **6**. When the loading ratio of **6** was 2 and 5 wt %, the gel points migrated slightly to lower temperature at $303\text{ }^\circ\text{C}$ and $285\text{ }^\circ\text{C}$, respectively (Fig. 7). This means the process window of the **5/6** mixture is about $70\text{--}88\text{ }^\circ\text{C}$ relying on the diamine inclusion. The values are comparable to those of many phthalonitrile monomers such as BZBPh

[19b], 3b-c [39], and 4M-P [3b], but still lower than those of the RTM-processable resins like RPh [7a], N = 2 [33], TDPE [13b], and HSiPN-ViSiPN [17] (see Table S5, column **Process window**). After gelation, the viscosity of the mixture increased abruptly as soon as the temperature was elevated to $275\text{ }^\circ\text{C}$. Intriguingly, the viscosity then exhibited a steady trend from $300\text{ }^\circ\text{C}$ to $350\text{ }^\circ\text{C}$, possibly because the increasing temperature generally drives the viscosity declined, simultaneously suppresses the curing rate (see Fig. 8a, blue curve). This steady trend may be interpreted as a compromise between the two factors. When the temperature exceeded $350\text{ }^\circ\text{C}$, the viscosity rose significantly again, implying the curing rate renewedly increased.

Subsequently, the complex viscosity as a function of phthalonitrile polymerization reaction was also investigated by conducting isothermal rheometric measurements at different temperatures on oligomer **5** with various concentrations of catalyst **6** (Fig. 8). All the prepolymers initially exhibited a melt viscosity of less than $20\text{ Pa}\cdot\text{s}$. The gelation occurred ranging from 7.2 min to 40.9 min. This step would be favorable for their meltability and processability. Specially, as displayed in Fig. 8a, after gelation, the slope of the increase of the viscosity fell as the maintained temperature, which exceeded $250\text{ }^\circ\text{C}$, increased. It indicates that those temperature ($>280\text{ }^\circ\text{C}$) would be disadvantageous to the cross-linking of **5/6** mixture, probably caused by the volatility or degradation of diamine **6** [15a]. Fig. 8b, c, d depict the complex viscosity correlated with time at 235 , 250 , $280\text{ }^\circ\text{C}$ distinguished by the diamine loading, respectively. Interestingly, the gelation time was negatively dependent on the ratio of the diamine at $235\text{ }^\circ\text{C}$ and $250\text{ }^\circ\text{C}$ (Fig. 8bc). To the best of our knowledge, this phenomenon has not appeared in any other works. A possible explanation would be that the bulky volume of the phenyl-*s*-triazine-containing prepolymer has hindered the further polymerization occurred between the prepolymer molecules; rather, the more mass ratio of diamine was added, the more bulky chains were generated. The interaction between the bulky chains should leap over the high potential energy, thus visibly resulting in delayed gelation (as Fig. 9 depicts). When

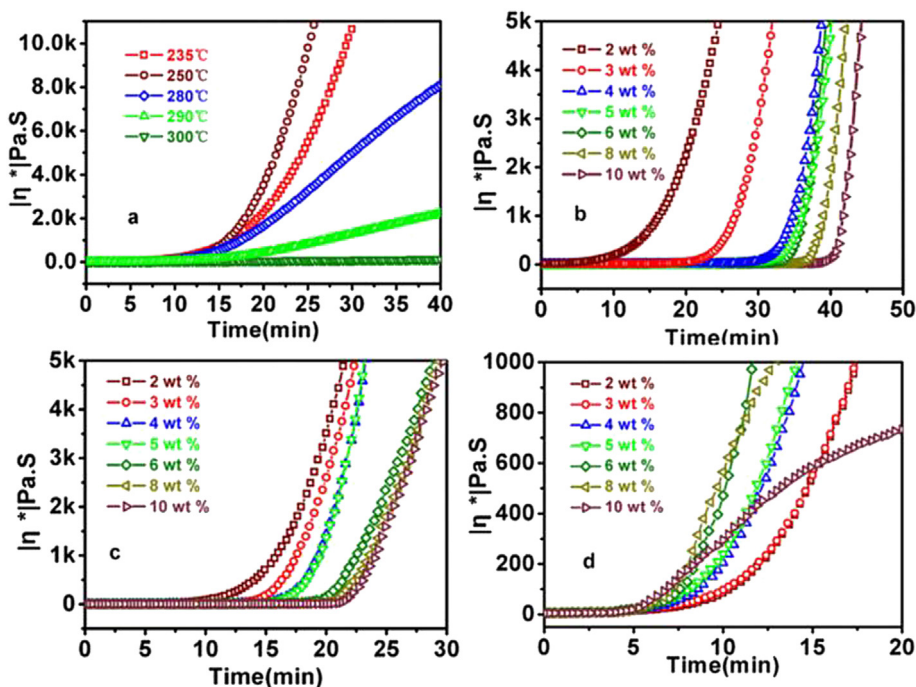


Fig. 8. Complex viscosity (η^*) of oligomer **5** with different mass ratios of diamine **6** as a function of time at various temperature: (a) 2 wt % **6** at various temperature; (b) with different mass ratios of **6** at $235\text{ }^\circ\text{C}$; (c) with different mass ratios of **6** at $250\text{ }^\circ\text{C}$; (d) with different mass ratios of **6** at $280\text{ }^\circ\text{C}$.

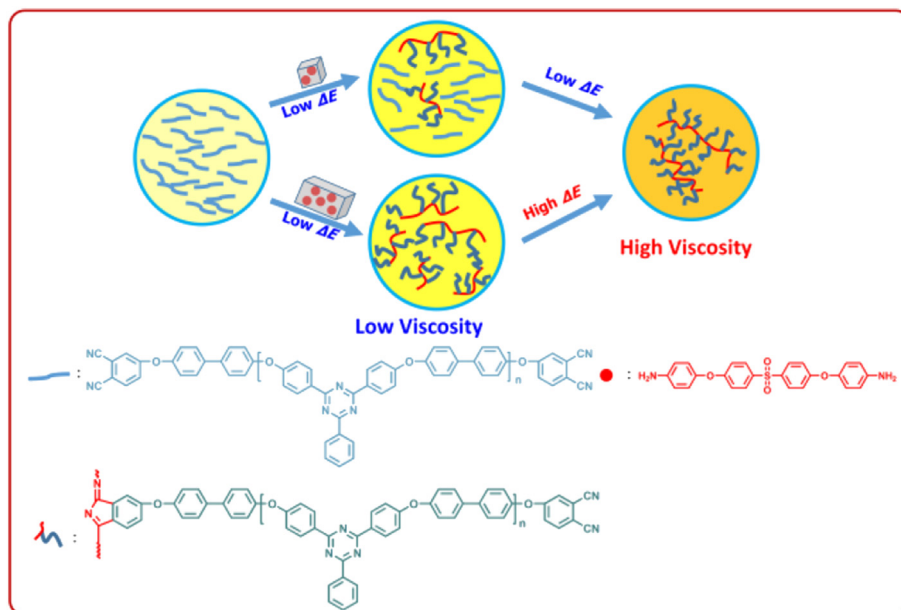


Fig. 9. The proposed graphical mechanism of the formation of the prepolymer.

the temperature was maintained at 280 °C (Fig. 8d), the reaction potential barrier was overwhelmed, the gelation time eventually increased linearly with diamine mass fraction. The rheological behaviors of 5/6 system reveal that the rate of their polymerization could be controlled by varying the diamine concentration or temperature. This would be a key factor that advantageously affects their processability through molding or lamination technology.

3.5. Thermal and thermo-oxidative stability

The thermal and thermo-oxidative stabilities of the networks (7) prepared by schedule c were investigated by TGA analysis. The relevant thermograms are presented in Figs. 10 and 11, respectively. The data are summarized in Table S3. The samples distinguished by diamine loading from 2 to 10 wt % showed the weight retention of 95% at 530–555 °C under N₂ atmosphere, and at 539–552 °C under a flow of air. The residue mass of the polymers ranged from 64 to 74%, when they are heated to 900 °C in N₂. The relative aerobic char yields for 7 are from 3 to 31% at 800 °C. These values show that all

the polymers possess excellent thermal and thermo-oxidative stabilities, which increase on the addition of 6. The fact is ascribed to the corresponding increase of the cross-linking density driven by the increasing 6 inclusion. Furthermore, owing to the presence of the thermally stable phenyl-*s*-triazine units in the polymer backbone, these thermal data are higher than those of many cured poly(aryl ether)-based phthalonitrile networks (e.g., PAEK-CN [40], PEN-t-BAPh [21a], 2CN-o-PEEK [21c], and also several oligomers disclosed by Keller [3f,9,33,41]), the ether-linked monomers (e.g., BDS [42], BPh, BAPh, 6FPH [15b], RPh [7a], and monomers 1–3 [16b]), and the self-curable monomers (e.g., 2O-P [16a], 3a-b [39], and 4O-M [3b]), but slightly lower than those of the cured TDPE [13b] and silane-bearing HSiPN-ViSiPN [17] (The corresponding thermal data of the reported networks are summarized in Table S5). However, a certain length of the molecular chain of 5 lowers the cross-linking density of 7 as compared to the above mentioned phthalonitrile monomers, which weakens the role of phenyl-*s*-triazine groups, in turn to lower the thermal stabilities of

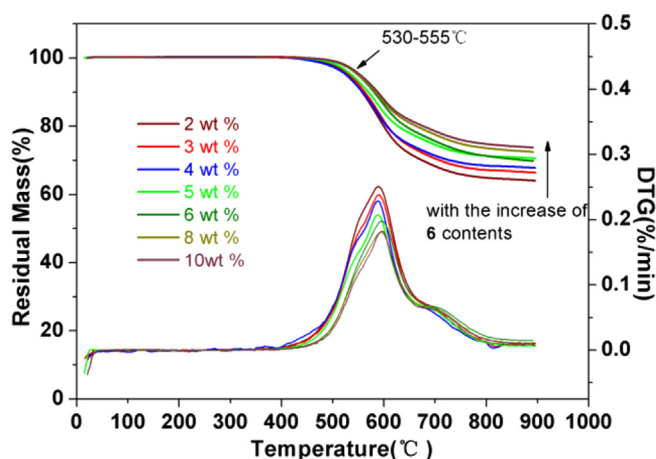


Fig. 10. TGA and DTG thermograms of the networks (7) after cured with different mass ratios of 6 under N₂ atmosphere.

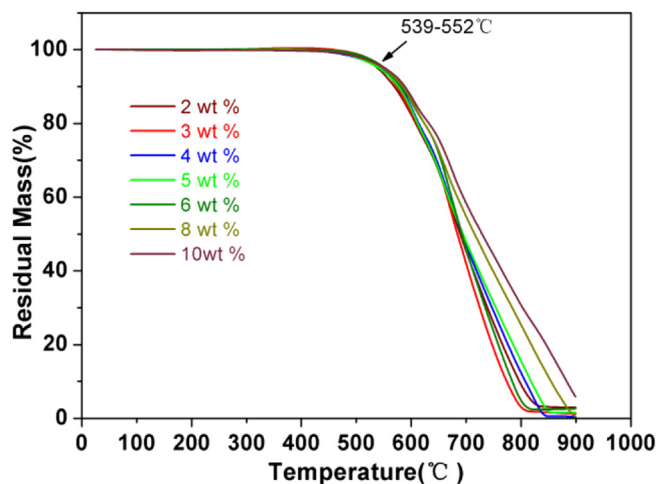


Fig. 11. TGA thermograms of the networks 7 after cured with different mass ratios of 6 under air atmosphere.

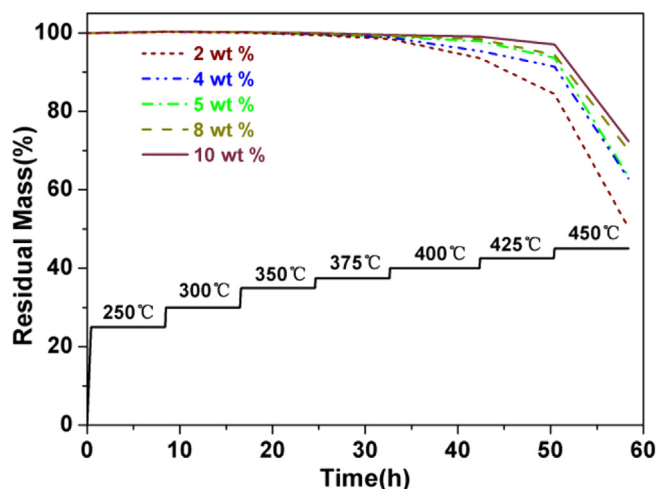


Fig. 12. Oxidative aging of networks (7) cured with different mass ratios of 6 after an approximately 60-h treatment at various temperatures.

the networks. The DTG curves disclose that these polymers undergo catastrophic failure at around 590 °C under N₂ atmosphere, while two stages of decomposition at temperatures about 590 °C and 660 °C was found with an atmosphere of flowing air, implying two different decomposition mechanisms. Research into the decomposition mechanisms is already underway.

The oxidative stabilities of the polymers were evaluated at various temperatures (to a maximum of 450 °C) each for 8-h intervals under ambient atmosphere (Fig. 12). The results showed that the thermosets (7) retained 50–72% of their initial weight varied by the 6 contents after the approximately 60-h period treatment. It was noteworthy that no distinct mass loss (0.5–1.5 wt %) could be observed during the 375 °C-treatment. The results could be roughly comparable to those of the famous PMR-II-30/Celion 6000 laminates [43] (aging at 371 °C for 200 h, mass loss for 12.5 wt %). The oxidative stabilities of 7s increase with the increase of diamine concentrations corresponding to the increasing cross-link density, which is consistent with their thermal stabilities detected by TGA. Note that the sulfur loss is higher than other elements after separately treated at steplike temperatures (i.e., 375, 425, 450 °C) as evidenced by the elemental analysis (Table S4,

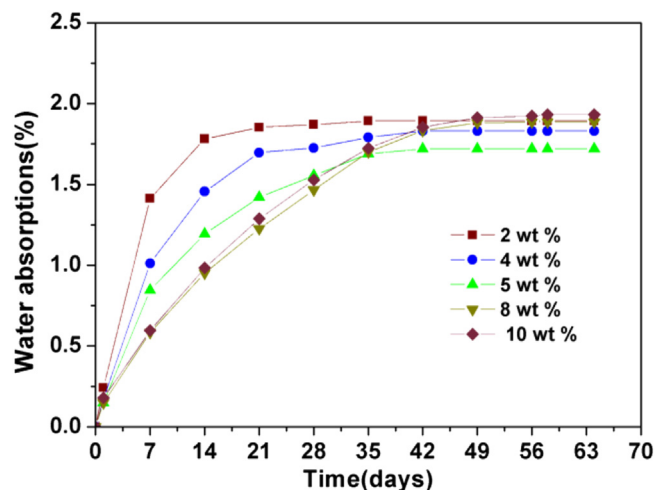


Fig. 13. Water absorption ratios of networks (7) cured with different mass ratios of 6 versus time at ambient temperature.

Fig. S13), strongly implying sulfur-containing diamine units are thermally weak segments in polymer components. We can further envision to load diamine with high-temperature-resistance structure as additive to pursue phthalonitrile resins which could be used at higher temperature (such as 450 °C) for long term (>200 h).

3.6. Water absorption capability

The water absorption capability of 7s was conducted with a sample soaked in distilled water at the ambient temperature (Fig. 13). The hygroscopicity of all the networks reached a maximum amount of 1.72–1.93 wt % over the course of approximately 65 days. The water absorption decreases as the levels of diamine concentrations increase toward 5 wt %. This is because the increasing cross-linking density hampered the osmosis of hydrone into polymer chains. Irregularly, the water absorption for the networks (8–10% diamine mass ratio) ultimately saturated at 1.89% and 1.93% after a 56-day immersion, respectively. This is thought as a result of the increasing amino groups in polymer backbone which would incur increasing hydrophilic capacity of the networks. Compared to other phthalonitrile counterparts [7b,42], the limited water absorption will definitely benefit the polymers 7 for applying at a high-humidity or aqueous environment.

3.7. Mechanical properties of network 7s/CF laminates

Dynamic mechanical analysis (DMA) was used to investigate the

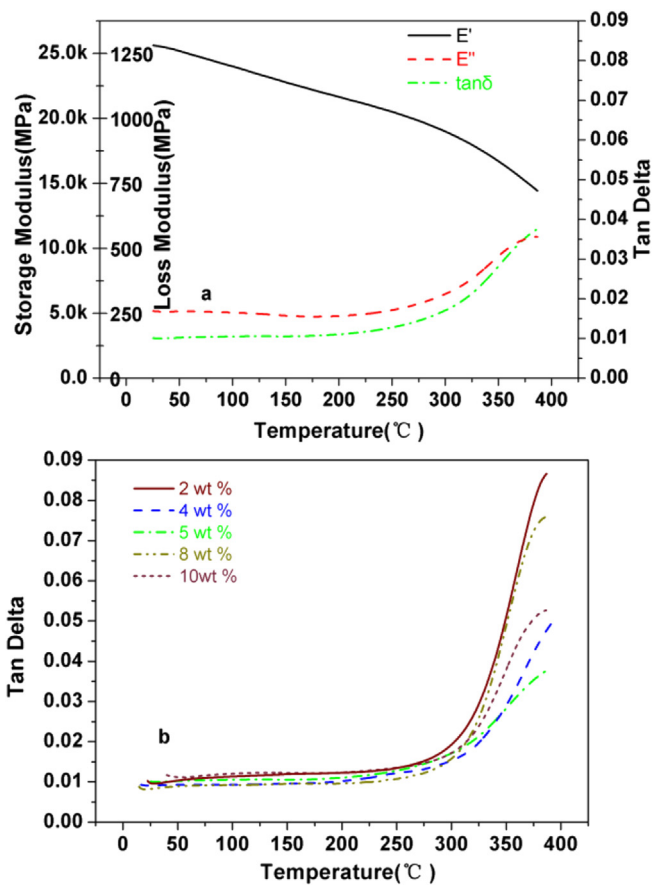


Fig. 14. DMA traces of networks 7/CF fabric composites cured with various concentrations of diamine 6: (a) E' , E'' and $\tan \delta$ of 5 wt % diamine containing 7 composites as a function of temperature; (b) $\tan \delta$ as a function of temperature with respect to the 6 concentrations.

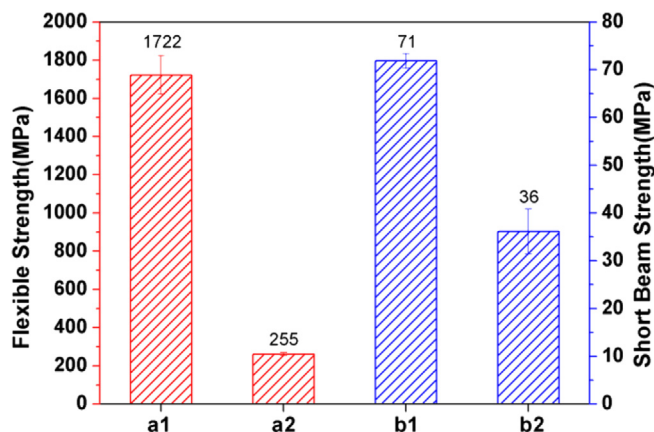


Fig. 15. Flexural strength (a) and interlaminar shear strength (b) of 7/CF laminate at ambient temperature (1) or 450 °C (2), respectively.

thermal properties of the composite laminates derived from the networks **7** and T300 CF fabric (The details of fabricating composite laminates are provided in [Supplementary data](#)). The corresponding DMA profiles are given in [Fig. 14](#). Taking the composites of 5 wt % addition network **7** as representative, the storage modulus fell with the temperature increased, and retained 14.5 GPa, 57% of its initial storage modulus, at 400 °C. Simultaneously, the $\tan \delta$ value peaked at around 400 °C, related to the glass transition of the polymer. [Fig. 14b](#) depicts the $\tan \delta$ traces of all the composites versus temperature. When the diamine inclusion was 5 wt %, the $\tan \delta$ exhibits the lowest height, indicating a minimum loss of its mechanical property. However, not any complete $\tan \delta$ peaks could be obtained from [Fig. 14](#). In order to determine the T_g of **7s**, high

temperature DSC tests were performed on the thermoset **7s** ([Fig. S15](#)). The results disclose that the T_g s of **7s** were from 418 to 424 °C. High diamine loading (6 wt%–10 wt%) would caused a slight decrease of T_g . Compared to the poly(aryl ether)-based phthalonitrile oligomers like PAEK-CN [40], PEN-t-Ph [44], 2CN-o-PEEK [21c], PEN-CN3 [45], and **6** [7b], the T_g s of **7s** are higher than those of phthalonitrile thermosets ([Table S5](#), column T_g). This is resulted from the contribution of the high-stiff phenyl-*s*-triazine moieties to the rigidity of the polymer backbone. As expected, the overall thermal properties of the networks (**7**) are significantly promoted by cooperating phenyl-*s*-triazine moieties into the polymer architecture.

Based on the DMA results, the network **7** comprising of 5 wt % diamine was selected to reinforce with continuous T700 carbon fiber. The mechanical property of the resulting composite laminate was evaluated according to ASTM D790M standard and ISO 14130 standard ([Fig. 15](#)). It was observed that the composite exhibited excellent mechanical property with the flexure strength of 1722 MPa and the interlaminar shear strength of 71 MPa at ambient temperature. When detected on-line at 450 °C, these values retained 15% and 51% of their initial values for 255 MPa and 36 MPa, respectively. The performance is a little disappointing, and probably results from a combined effect of superabundant ether linkage encompassed in polymer framework and a certain length of the polymer main chain, both of which would encourage the mobility of the main chain of the networks. For some positive aspects, the data at 450 °C would be a reference in further research. Successively, scanning electron microscopy (SEM) studies were performed on the surfaces of the cracked samples to assess the failure mechanism. Room-temperature failure ([Fig. 16ab](#)) underwent a co-break process, accompanied by a little extraction of CF from resins (white arrows). The fracture morphology of the resin phase is smooth (red arrows), indicating a brittle cracked mechanism. In contrast, when

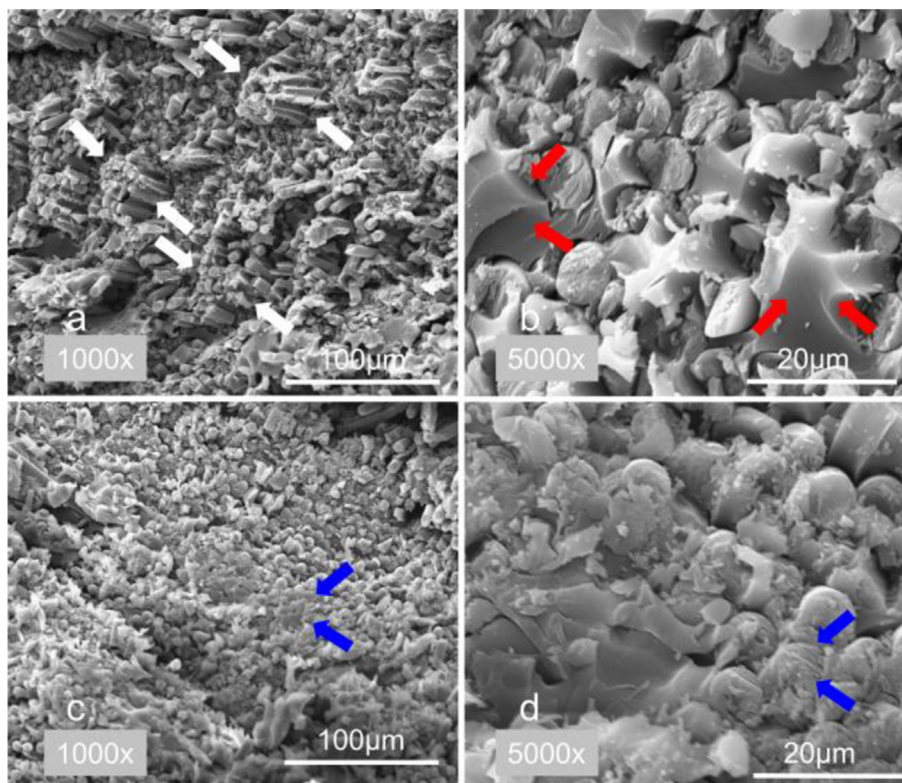


Fig. 16. The cross-sectional images for the network **7**/CF laminate broken at ambient temperature (a, b) or 450 °C (c, d) monitored by SEM instrument.

laminates were broken at 450 °C, the fracture surface was coarse, and the resins covered the cross section of the fiber (Fig. 16cd, blue arrows). However, the interfacial adhesion between **7** and CF is just physical connection which could be easily broken; thus, enhancing the interfacial strength *via* chemically modifying the surface of fibers is necessary. The work is underway and will be reported in the future.

4. Conclusion

This paper mainly discussed the synthesis, cross-linking, physical properties, and advanced applications of novel phenyl-s-triazine-containing phthalonitrile resins. The preparation of oligomeric precursor was achieved by a two-step, one-pot reaction with high yields. Diamine **6** was added to elevate the curing rate, and the diamine concentration and the temperature could readily control the gelation time. The curing schedule was subsequently optimized to give high cross-linking density networks with excellent thermal and mechanical properties. The resulting networks (**7**) all possessed high glass transition temperature at around 400 °C, outstanding thermal and thermo-oxidative stability as well as limited water absorption (1.72–1.93 wt %). The **7**/CF composite materials exhibited high flexural strength of 1722 MPa and interlaminar shear strength of 71 MPa at ambient temperature. The retention of value at 450 °C was 15% and 51%, respectively. All of the merits displayed above obviously suggest that the phenyl-s-triazine-bearing phthalonitrile resins are qualified for the applications as high temperature structural materials.

Acknowledgments

We thank the National High Technology Research and Development Program (“863”Program) of China (Nos. 2015AA033802) and the National Science Foundation of China (Nos. 21074017).

Appendix A. Supplementary data

Supplementary data related to this article can be found at <http://dx.doi.org/10.1016/j.polymer.2015.09.035>.

References

- [1] (a) T. Agag, J. Liu, R. Graf, H.W. Spiess, H. Ishida, *Macromolecules* 45 (22) (2012) 8991–8997; (b) M. Naffakh, A.M. Diez-Pascual, C. Marco, G.J. Ellis, M.A. Gomez-Fatou, *Prog. Polym. Sci.* 38 (8) (2013) 1163–1231; (c) C. Tridech, H.A. Maples, P. Robinson, A. Bismarck, *ACS Appl. Mat. Interfaces* 5 (18) (2013) 9111–9119; (d) M. Antunes, J.I. Velasco, *Prog. Polym. Sci.* 39 (3) (2014) 486–509; (e) I. Hamerton, L.T. McNamara, B.J. Howlin, P.A. Smith, P. Cross, S. Ward, *Macromolecules* 47 (6) (2014) 1935–1945.
- [2] (a) D.M. Wu, Y.C. Zhao, K. Zeng, G. Yang, *J. Polym. Sci. Part A Polym. Chem.* 50 (23) (2012) 4977–4982; (b) X.Q. Zou, M.Z. Xu, K. Jia, X.B. Liu, *J. Appl. Polym. Sci.* 131 (23) (2014) 41203–41209; (c) K. Zeng, Y. Zou, G. Yang, *Des. Monomers Polym.* 17 (2) (2014) 186–193; (d) J. Hu, Y. Liu, Y. Jiao, S. Ji, R. Sun, P. Yuan, K. Zeng, X. Pu, G. Yang, *RSC Adv.* 5 (21) (2015) 16199–16206; (e) P. Yuan, Y. Liu, K. Zeng, G. Yang, *Des. Monomers Polym.* 18 (4) (2015) 343–349.
- [3] (a) D.D. Dominguez, T.M. Keller, *Polymer* 48 (2007) 91–97; (b) B. Amir, H. Zhou, F. Liu, H. Aurangzeb, *J. Polym. Sci. Part A Polym. Chem.* 48 (24) (2010) 5916–5920; (c) M. Laskoski, A. Neal, T.M. Keller, D. Dominguez, C.A. Klug, A.P. Saab, *J. Polym. Sci. Part A Polym. Chem.* 52 (12) (2014) 1662–1668; (d) Y. Zhan, X. Yang, H. Guo, J. Yang, F. Meng, X. Liu, *J. Mater. Chem.* 22 (12) (2012) 5602–5608; (e) H. Guo, Y. Zhan, Z. Chen, F. Meng, J. Wei, X. Liu, *J. Mater. Chem. A* 1 (6) (2013) 2286–2296; (f) M. Laskoski, D.D. Dominguez, T.M. Keller, *J. Polym. Sci. Part A Polym. Chem.* 51 (22) (2013) 4774–4778.
- [4] C.S. Marvel, J.H. Rassweiler, *J. Am. Chem. Soc.* 80 (5) (1958) 1197–1199.
- [5] (a) T.M. Keller, J.R. Griffith, *Abstr. Pap. Am. Chem. S* 176 (1978) 105–106; (b) T.M. Keller, J.R. Griffith, *J. Fluor. Chem.* 13 (4) (1979) 315–324.
- [6] (a) T.M. Keller, T.R. Price, *J. Macromol. Sci. A* 18 (6) (1982) 931–937; (b) T.M. Keller, *Polymer* 34 (5) (1993) 952–955; (c) M.L. Warzel, T.M. Keller, *Polymer* 34 (3) (1993) 663–666; (d) M. Laskoski, T.M. Keller, S.B. Qadri, *Polymer* 48 (26) (2007) 7484–7489.
- [7] (a) T.M. Keller, D.D. Dominguez, *Polymer* 46 (13) (2005) 4614–4618; (b) M. Laskoski, D.D. Dominguez, T.M. Keller, *J. Polym. Sci. Part A Polym. Chem.* 43 (18) (2005) 4136–4143.
- [8] (a) S.B. Sastri, J.P. Armistead, T.M. Keller, *Polym. Compos.* 17 (6) (1996) 816–822; (b) S.B. Sastri, J.P. Armistead, T.M. Keller, U. Sorathia, *Polym. Compos.* 18 (1) (1997) 48–54; (c) D.D. Dominguez, H.N. Jones, T.M. Keller, *Polym. Compos.* 25 (5) (2004) 554–561.
- [9] T.M. Keller, *Chem. Mater.* 6 (1994) 302–305.
- [10] (a) R.P. Linstead, A.R. Lowe, *J. Chem. Soc.* (1934) 1022–1027; (b) T.R. Walton, J.R. Griffith, *Abstr. Pap. Am. Chem. S* 169 (1975) 98.
- [11] Y.Z. Meng, I.A. Abu-Yousef, A.R. Hlil, A.S. Hay, *Macromolecules* 33 (25) (2000) 9185–9191.
- [12] (a) A.W. Snow, J.R. Griffith, N.P. Marullo, *Macromolecules* 17 (8) (1984) 1614–1624; (b) K. Zeng, K. Zhou, S. Zhou, H. Hong, H. Zhou, Y. Wang, P. Miao, G. Yang, *Eur. Polym. J.* 45 (4) (2009) 1328–1335; (c) Z. Chen, X. Yang, M. Xu, X. Liu, *High. Perform. Polym.* 26 (1) (2013) 3–11.
- [13] (a) P.J. Burchill, *J. Polym. Sci. Part A Polym. Chem.* 32 (1) (1994) 1–8; (b) H. Sheng, X. Peng, H. Guo, X. Yu, C. Tang, X. Qu, Q. Zhang, *Mater. Chem. Phys.* 142 (2–3) (2013) 740–747.
- [14] D. Augustine, D. Mathew, C.P. Reghunadhan Nair, *Polymer* 60 (0) (2015) 308–317.
- [15] (a) S.B. Sastri, T.M. Keller, *J. Polym. Sci. Part A Polym. Chem.* 36 (11) (1998) 1885–1890; (b) S.B. Sastri, T.M. Keller, *J. Polym. Sci. Part A Polym. Chem.* 37 (13) (1999) 2105–2111.
- [16] (a) H. Zhou, A. Badashah, Z. Luo, F. Liu, T. Zhao, *Polym. Adv. Technol.* 22 (10) (2011) 1459–1465; (b) A. Badshah, M.R. Kessler, H. Zhou, A. Hasan, *Polym. Int.* 63 (3) (2014) 465–469.
- [17] Z.B. Zhang, Z. Li, H. Zhou, X.K. Lin, T. Zhao, M.Y. Zhang, C.H. Xu, *J. Appl. Polym. Sci.* 131 (20) (2014).
- [18] (a) D.D. Dominguez, T.M. Keller, *J. Appl. Polym. Sci.* 110 (4) (2008) 2504–2515; (b) H. Guo, Y. Zou, Z. Chen, J. Zhang, Y. Zhan, J. Yang, X. Liu, *High. Perform. Polym.* 24 (7) (2012) 571–579; (c) X. Zhao, Y. Lei, R. Zhao, J. Zhong, X. Liu, *J. Appl. Polym. Sci.* 123 (6) (2012) 3580–3586; (d) X. Zhao, H. Guo, Y. Lei, R. Zhao, J. Zhong, X. Liu, *J. Appl. Polym. Sci.* 127 (6) (2013) 4873–4878.
- [19] (a) Z. Brunovska, R. Lyon, H. Ishida, *Thermochim. Acta* 357–358 (2000) 195–203; (b) F. Zuo, X. Liu, *J. Appl. Polym. Sci.* 117 (3) (2010) 1469–1475.
- [20] (a) M.J. Sumner, M. Sankarapandian, J.E. McGrath, J.S. Riffle, U. Sorathia, *Polymer* 43 (19) (2002) 5069–5076; (b) H. Guo, Y. Lei, X. Zhao, X. Yang, R. Zhao, X. Liu, *J. Appl. Polym. Sci.* 125 (1) (2012) 649–656; (c) B. Zhang, Z. Luo, H. Zhou, F. Liu, R. Yu, Y. Pan, Y. Wang, T. Zhao, *High Perform. Polym.* 24 (5) (2012) 398–404; (d) D. Augustine, D. Mathew, C.P.R. Nair, *Polym. Int.* 64 (1) (2015) 146–153.
- [21] (a) R. Du, W. Li, X. Liu, *Polym. Degrad. Stab.* 94 (12) (2009) 2178–2183; (b) X. Yang, J. Zhang, Y. Lei, J. Zhong, X. Liu, *J. Appl. Polym. Sci.* 121 (4) (2011) 2331–2337; (c) H. Zhang, T. Liu, W. Yan, Y. Su, H. Yu, Y. Yang, Z. Jiang, *High Perform. Polym.* 26 (8) (2014) 1007–1014.
- [22] K. Zeng, H.B. Hong, S.H. Zhou, D.M. Wu, P.K. Miao, Z.F. Huang, G. Yang, *Polymer* 50 (21) (2009) 5002–5006.
- [23] (a) T.M. Keller, *Polymer* 34 (1993) 952–955; (b) P. Selvakumar, M. Sarojadevi, P. Sundararajan, *Mater. Sci. Eng. B ADV* 168 (1–3) (2010) 214–218.
- [24] (a) M. Xu, X. Shi, X. Zou, H. Pan, M. Liu, K. Jia, X. Liu, *J. Magn. Mater.* 371 (2014) 20–28; (b) L.F. Tong, Z.J. Pu, Z.R. Chen, X. Huang, X.B. Liu, *Polym. Compos.* 35 (2) (2014) 344–350; (c) M. Liu, K. Jia, X. Liu, *J. Appl. Polym. Sci.* 132 (10) (2015) 41595–41602; (d) T.M. Robert, D. Augustine, S.M. Chandran, D. Mathew, C.P.R. Nair, *RSC Adv.* 5 (2) (2015) 1198–1204; (e) K. Jia, P. Wang, L. Yuan, X. Zhou, W. Chen, X. Liu, *J. Mater. Chem. C* 3 (15) (2015) 3522–3529; (f) F. Meng, X. Liu, *RSC Adv.* 5 (10) (2015) 7018–7022.
- [25] G.P. Yu, C. Liu, X.P. Li, J.Y. Wang, X.G. Jian, C.Y. Pan, *Polym. Chem.* 3 (4) (2012) 1024–1032.
- [26] G.P. Yu, J.Y. Wang, C. Liu, E.C. Lin, X.G. Jian, *Polymer* 50 (7) (2009) 1700–1708.
- [27] C. Liu, J.Y. Wang, E.C. Lin, L.S. Zong, X.G. Jian, *Polym. Degrad. Stab.* 97 (3) (2012) 460–468.
- [28] (a) G.P. Yu, J.Y. Wang, C. Liu, E.C. Lin, X.G. Jian, *Polymer* 50 (2009) 1700–1708; (b) G.P. Yu, C. Liu, J.Y. Wang, G.H. Li, Y.J. Han, X.G. Jian, *Polymer* 51 (1) (2010)

- 100–109.
- [29] (a) D.M. Tigelaar, A.E. Palker, C.M. Jackson, K.M. Anderson, J. Wainright, R.F. Savinell, *Macromolecules* 42 (6) (2009) 1888–1896;
(b) D.M. Tigelaar, A.E. Palker, R.H. He, D.A. Scheiman, T. Petek, R. Savinell, M. Yoonessi, *J. Membr. Sci.* 369 (1–2) (2011) 455–465.
- [30] (a) S. Matsuo, *J. Polym. Sci. Part A Polym. Chem.* 32 (11) (1994) 2093–2098;
(b) R. Fink, C. Frenz, M. Thelakkat, H.W. Schmidt, *Macromolecules* 30 (26) (1997) 8177–8181;
(c) R. Fink, Y. Heischkel, M. Thelakkat, H.W. Schmidt, C. Jonda, M. Huppaufl, *Chem. Mater* 10 (11) (1998) 3620–3625.
- [31] M. Barikani, S. Mehdipour–Ataei, *J. Polym. Sci. Part A Polym. Chem.* 38 (9) (2000) 1487–1492.
- [32] R. Singh, A.S. Hay, *Macromolecules* 25 (3) (1992) 1025–1032.
- [33] D.D. Dominguez, T.M. Keller, *High Perform. Polym.* 18 (3) (2006) 283–304.
- [34] (a) T.M. Keller, T.R. Price, J.R. Griffith, *Abstr. Pap. Am. Chem. S* 180 (1980) 165–166, Aug;
(b) T.M. Keller, *J. Polym. Sci. Part A Polym. Chem.* 26 (12) (1988) 3199–3212.
- [35] H.E. Kissinger, *Anal. Chem.* 29 (11) (1957) 1702–1706.
- [36] Z.S. Guo, S.Y. Du, B.M. Zhang, Z.J. Wu, *J. Appl. Polym. Sci.* 92 (5) (2004) 3338–3342.
- [37] J.K. Herman Teo, K.C. Teo, B. Pan, Y. Xiao, X. Lu, *Polymer* 48 (19) (2007) 5671–5680.
- [38] Y.Y. Han, G.X. Liao, Y.J. Xu, G.P. Yu, X.G. Jian, *Polym. Eng. Sci.* 49 (12) (2009) 2301–2308.
- [39] A. Badshah, M.R. Kessler, H. Zhou, J.H. Zaidi, S. Hameed, A. Hasan, *Polym. Chem.* 4 (12) (2013) 3617–3622.
- [40] T. Liu, Y. Yang, T. Wang, H. Wang, H. Zhang, Y. Su, Z. Jiang, *Polym. Eng. Sci.* 54 (7) (2014) 1695–1703.
- [41] M. Laskoski, D.D. Dominguez, T.M. Keller, *Polymer* 48 (21) (2007) 6234–6240.
- [42] X. Peng, H. Sheng, H. Guo, K. Naito, X. Yu, H. Ding, X. Qu, Q. Zhang, *High Perform. Polym.* 26 (7) (2014) 837–845.
- [43] R.D. Vannucci, *Sampe Q. Soc. Adv. Mater. Process Eng.* 19 (1) (1987) 31–36.
- [44] Y. Zou, J. Yang, Y. Zhan, X. Yang, J. Zhong, R. Zhao, X. Liu, *J. Appl. Polym. Sci.* 125 (5) (2012) 3829–3835.
- [45] J. Yang, X.L. Yang, Y.K. Zou, Y.Q. Zhan, R. Zhao, X.B. Liu, *J. Appl. Polym. Sci.* 126 (3) (2012) 1129–1135.